Syntheses, Structure, and Reactivity of Chiral Titanium Compounds: Procatalysts for Olefin Polymerization

Piotr Sobota,*[a] Katarzyna Przybylak,[a] Józef Utko,[a] Lucjan B. Jerzykiewicz,[a] Armando J. L. Pombeiro,[b] M. Fátima C. Guedes da Silva,[b, c] and Krzysztof Szczegot[d]

Abstract: Titanium complexes with chelating alkoxo ligands have been synthesised with the aim to investigate titanium active centres in catalytic ethylene polymerisation. The titanium complexes *cis*-[$TiCl_2(\eta^2$-maltolato$)_2$] (**1**, 89%), and *cis*-[$TiCl_2(\eta^2$-guaiacolato$)_2$] (**2**, 80%) were prepared by direct reaction of $TiCl_4$ with maltol and guaiacol in toluene. The addition of maltol to [Ti(O*i*Pr)$_4$] in THF results in the formation of species [Ti(O*i*Pr)$_2$(maltolato)$_2$] (**3**, 82%). The titanium compound *cis*-[$Ti(OEt)_2(\eta^2$-maltolato$)_2$] (**4**, 74%) was obtained by the transesterification reaction of species **3** with CH_3CO_2Et. When compound **4** is dissolved in THF a dinuclear species [$Ti_2(\mu$-OEt$)_2$(OEt$)_4$-(η^2-maltolato$)_2$] (**5**, 45%) is formed. Reaction of [Ti(O*i*Pr)$_4$] with crude guaiacol in THF yields a solid, which after recrystallisation from acetonitrile gives [$Ti_4(\mu$-O$)_4(\eta^2$-guaiacolato$)_8$]·$4CH_3CN$ (**6**, 55%). In contrast, reaction of $TiCl_4$ with crude guaiacol in tetrahydrofuran affords [$Ti_2(\mu$-O$)Cl_2(\eta^2$-guaiacolato$)_4$] (**7**, 82%). Crystallographic and electrochemical analyses of these complexes demonstrate that maltolato and guaiacolato ligands can be used as a valuable alternative for the cyclopentadienyl ring. These complexes have been shown to be active catalysts upon combination with the appropriate activator.

Keywords: alkenes · alkoxides · chirality · polymerization · titanium

Introduction

Metallocene-catalysed α-olefin polymerisation provides an excellent example for the understanding of the relationship between the geometry of the metal active site and its reactivity in homogeneous catalysis.[1] In order to extend the homogenous catalytic applications, current studies have been focused on non-metallocene systems based on dialkoxides[2] and diamido[3] ligands. For instance sterically hindered chelating biphenol and binaphthol complexes that possess C_2 symmetry can provide a stereochemically rigid framework for the metal centre.[4] The molecular structures of these chiral intermediates can provide explanations for their reactivity and selectivity, but relatively few structures of chiral non-metallocene titanium catalysts for olefin polymerisation are known.[5] As a part of a more general study of titanium complexes, which relate to the chiral single-site metal active centre in olefin polymerisation catalysts, we have reported the synthesis and crystal structure of the *cis*-[{$C_2H_4(CO_2Et)_2$}$_2Cl_2$Ti][$SbCl_6$]$_2$ salt.[6] In the *cis*-[{C_2H_4-(CO_2Et)$_2$}$_2Cl_2$Ti]$^{2+}$ ion, the chiral titanium atom is octahedrally coordinated by two mutually *cis* chlorine atoms and four carbonyl oxygen atoms of two chelating diethyl succinate molecules. To extend this chemistry we have been attempting to synthesise new titanium species with maltolato ((*O*,*O*)-3-oxy-2-methyl-pyran-4-onato) and guaiacolato ((*O*,*O*′)-2-methoxyphenoxo) ligands.

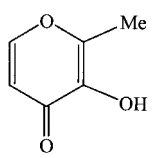

maltol

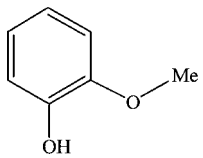

guaiacol

Here we describe the syntheses leading to compounds **1**–**7** and report details of their crystal structures, electrochemical studies and catalytic activity in ethylene and propylene polymerisation.

[a] Prof. Dr. P. Sobota, K. Przybylak, Dr. J. Utko, Dr. L. B. Jerzykiewicz
Faculty of Chemistry, University of Wrocław
14, F. Joliot-Curie, 50-383 Wrocław (Poland)
Fax: (+48) 71 3282348
E-mail: plas@wchuwr.chem.uni.wroc.pl

[b] Prof. Dr. A. J. L. Pombeiro, Dr. M. F. C. Guedes da Silva
Centro de Química Estrutural, Complexo I
Instituto Superior Técnico, Av. Rovisco Pais
1049-001 Lisboa (Portugal)

[c] Dr. M. F. C. Guedes da Silva
Universidade Lusófona de Humanidades e Tecnologias
Campo Grande, 376, 1749-024 Lisboa (Portugal)

[d] Dr. K. Szczegot
University of Opole 48 Oleska
45-342 Opole (Poland)

  0947-6539/01/0705-0951 $ 17.50+.50/0

Results and Discussion

Synthesis, properties and structural characterisation: We found that the direct reaction of $TiCl_4$ with maltol or freshly distilled guaiacol in a 1:2 molar ratio in toluene gives air-sensitive, but stable under dinitrogen, orange *cis*-[$TiCl_2(\eta^2$-maltolato$)_2$] (**1**) and brown-orange *cis*-[$TiCl_2(\eta^2$-guaiacolato$)_2$] (**2**) (Scheme 1).

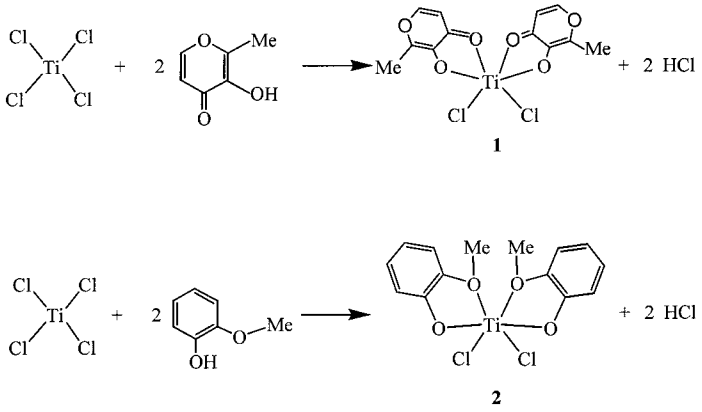

Scheme 1. Synthesis of **1** and **2**.

The addition of maltol to [Ti(O*i*Pr)$_4$] in a 2:1 molar ratio in THF results in the formation of [Ti(O*i*Pr)$_2(\eta^2$-maltolato$)_2$] (**3**). Up to now we have not been able to obtain **3** in a crystalline form. Thus, titanium species *cis*-[Ti(OEt)$_2(\eta^2$-maltolato$)_2$] (**4**) was obtained in the transesterification reaction of **3** with CH_3CO_2Et (Scheme 2). The transesterification reaction is one of the most important ways of manipulating the ester functionality as exemplified by many protocols that have been developed for carrying out this reaction.[7, 8] Compound **4** (see electrochemical studies) recrystallised from THF yields mixtures of crystals: cubic-shaped **4** and plate-shaped **5**.

Crystals of **1** consist of the *cis*-[$TiCl_2(\eta^2$-maltolato$)_2$] molecule and a THF solvate residing on a centre of inversion. Unfortunately, the THF molecule disorder could not be resolved and therefore the structure of **1** was not determined completely. Nonetheless the structure of **1** is clearly visible and can be discussed. Structures of **1, 2** and **4** are depicted in Figures 1, 2 and 3, respectively. In these complexes titanium

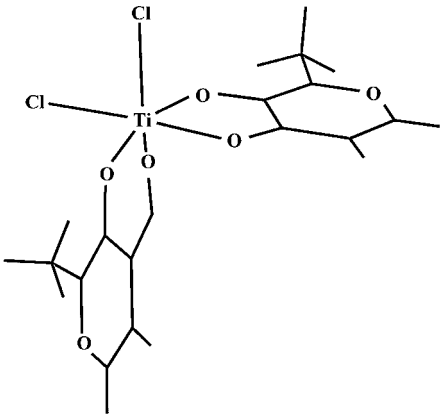

Figure 1. The drawing of *cis*-[$TiCl_2(\eta^2$-maltolato$)_2$] (**1**). Crystal data: monoclinic, $C2/c$, $a = 13.110(1)$, $b = 11.785(1)$, $c = 13.809(1)$ Å, $\beta = 117.48°$, $T = 100$ K.

atoms exhibit octahedral coordination and lie on a twofold axis. The titanium atoms in **1**, **2** and **4** are surrounded by four oxygen atoms of two chelating maltolato and guaiacolato ligands and by two mutually *cis* chlorine or OEt groups, respectively. The Ti–Cl and Ti–O bond lengths, in **2** and **4** are similar to those previously reported for [$TiCl_4\{C_2O_4$-$(CH_2CH_2Ph)_2\}$] and [$TiCl_4\{C_4H_7O(CO_2Et)\}_2$].[9–11] Compound **5** was shown by X-ray diffraction study to have a dimeric structure, and an overall view of the molecule is presented in Figure 4. Due to the presence of bidentate maltolato chelating agents, two bridging μ-OEt and two terminal, mutually *cis* OEt groups, the geometry at each Ti atom in **5** is chiral, and the molecule as a whole possesses C_2 symmetry. The terminal Ti–O(1)$_{ethoxide}$ (1.809(3) Å) and Ti–O(3)$_{ethoxide}$ (1.778(3) Å) bond lengths are comparable to Ti–O$_{ethoxide}$ bond lengths in **4**, but are shorter than the Ti-μ-O(2)$_{ethoxide}$ bond length of 1.969(3) Å in **5**.

The reaction course of TiX_4 (X = OR, Cl) with guaiacol is significantly changed by moisture. Treatment of [Ti(O*i*Pr)$_4$] with crude guaiacol in THF yields product, which after recrystallisation from acetonitrile can be isolated as crystalline material, [$Ti_4(\mu$–O$)_4(\eta^2$-guaiacolato$)_8$]·4CH_3CN (**6**; Scheme 3). The solid-state structure of **6** shown in Figure 5 consists of [$Ti_4(\mu$-O$)_4(\eta^2$-guaiacolato$)_8$] species and four CH_3CN solvent molecules of crystallisation. The Ti_4O_4 moiety is significantly distorted from planarity: the four titanium atoms and two oxygen atoms (O(1) and O(1a)) are within 0.027(1) Å of the plane, but the remaining oxygen

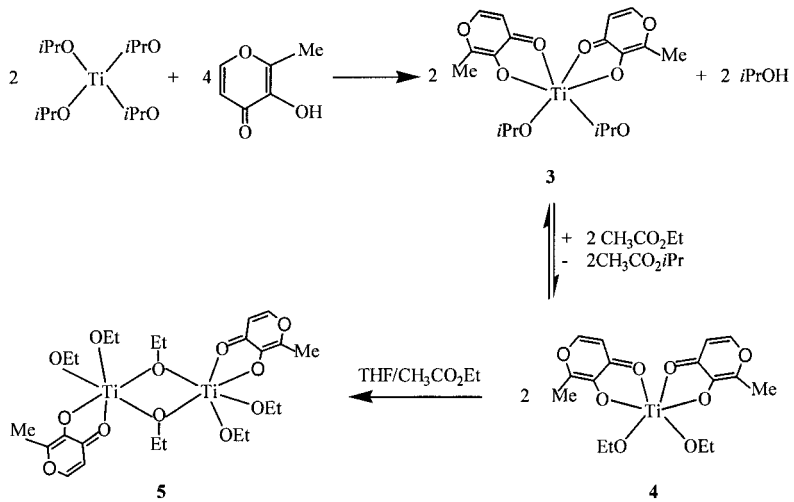

Scheme 2. Reaction scheme for the preparation of **3**, **4** and **5**.

0947-6539/01/0705-0952 $ 17.50+.50/0 *Chem. Eur. J.* **2001**, *7*, No. 5

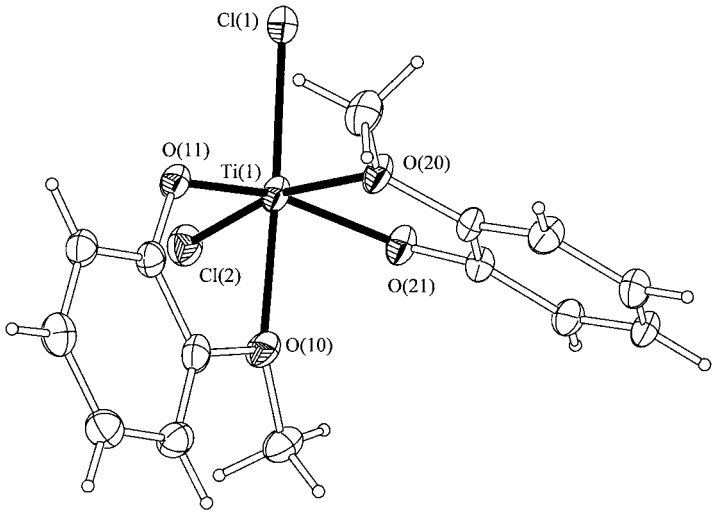

Figure 2. Molecular structure of *cis*-[$TiCl_2(\eta^2$-guaiacolato$)_2$] (**2**). The displacement ellipsoids are drawn at the 50% probability level. Selected bond lengths [pm] and angles [deg]: Ti(1)–Cl(1) 224.56(8), Ti(1)–Cl(2) 225.03(8), Ti(1)–O(10) 219.30(19), Ti(1)–O(11) 186.81(17), Ti(1)–O(20) 221.49(18), Ti(1)–O(21) 186.06(17), Ti(2)–Cl(3) 225.24(8), Ti(2)–Cl(4) 226.41(8), Ti(2)–O(30) 219.70(18), O(21)-Ti(1)-O(10) 81.80(8), O(11)-Ti(1)-O(10) 75.58(7), O(10)-Ti(1)-O(20) 81.06(7), O(21)-Ti(1)-Cl(1) 104.38(7), O(11)-Ti(1)-Cl(1) 95.35(6), O(10)-Ti(1)-Cl(1) 169.03(5), O(20)-Ti(1)-Cl(1) 91.70(5), O(21)-Ti(1)-Cl(2) 97.11(6), O(10)-Ti(1)-Cl(2) 90.30(5), Cl(1)-Ti(1)-Cl(2) 97.79(3).

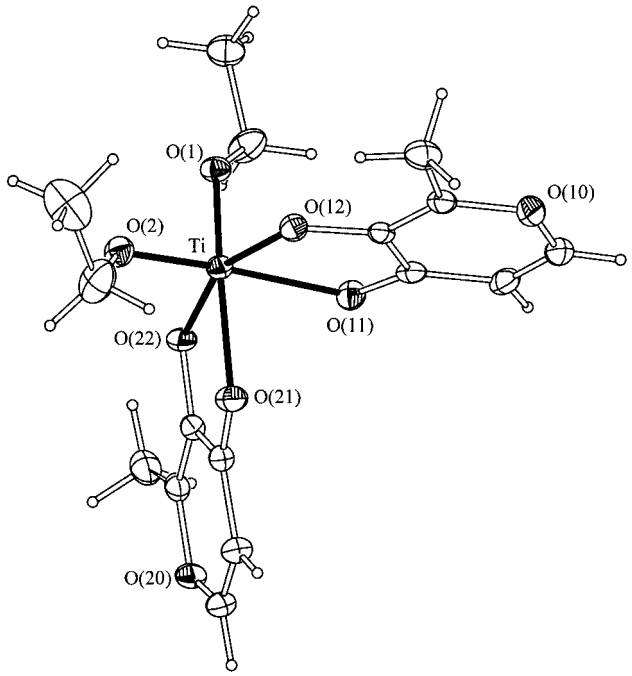

Figure 3. Molecular structure of *cis*-[$Ti(OEt)_2(\eta^2$-maltolato$)_2$] (**4**). The displacement ellipsoids are drawn at the 50% probability level. Selected bond lengths [pm] and angles [deg]: Ti–O(1) 179.64(14), Ti–O(2) 182.20(14), Ti–O(12) 197.90(14), Ti–O(22) 198.51(14), Ti–O(21) 211.30(14), Ti–O(11) 213.86(14), O(1)-Ti-O(2) 100.36(6), O(1)-Ti-O(12) 102.77(6), O(1)-Ti-O(22) 88.90(6), O(1)-Ti-O(21) 164.97(5), O(2)-Ti-O(21) 90.12(6), O(12)-Ti-O(21) 87.73(6), O(22)-Ti-O(21) 77.91(6).

atoms (O(2) and O(2a)) are 0.490(2) Å alternately above and below this plane. In **6**, the four titanium atoms have equivalent geometry. Each is bonded to four oxygen atoms of two coordinated guaiacolatos and two mutually *cis*-bridging oxy-

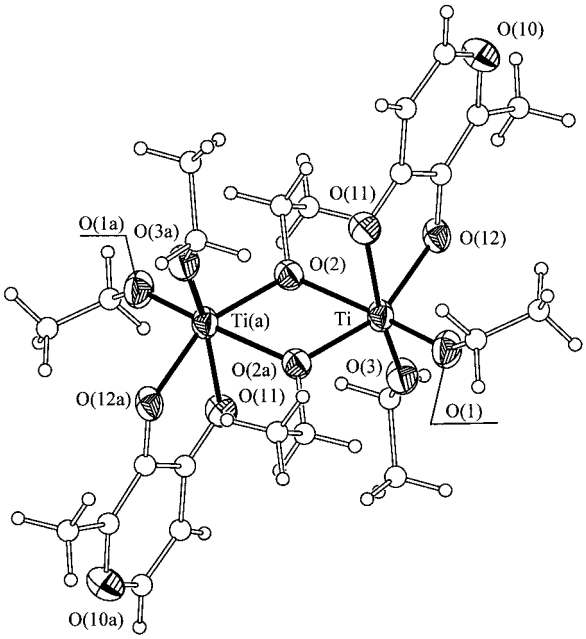

Figure 4. Molecular structure of [$Ti_2(\mu$-$OEt)_2(OEt)_4(\eta^2$-maltolato$)_2$] (**5**). The displacement ellipsoids are drawn at the 50% probability level. The second position of disordered carbon atoms of OEt groups are omitted for clarity. Selected bond lengths [pm] and angles [deg]: Ti–O(3) 177.8(3), Ti–O(1) 180.9(3), Ti–O(2a) 196.9(3), Ti–O(12) 197.3(3), Ti–O(2) 208.0(3), Ti–O(11) 2.171(3), O(3)-Ti-O(1) 96.71(13), O(3)-Ti-O(2a) 101.91(12), O(3)-Ti-O(12) 93.30(12), O(2a) -Ti-O(12) 156.65(11), O(1)-Ti-O(2) 165.72(12), O(2a)-Ti-O(2) 72.59(12), O(3)-Ti-O(11) 169.95(12), O(2a)-Ti-O(11) 87.43(11), O(12)-Ti-O(11) 76.67(10), O(2)-Ti-O(11) 84.60(10), Ti-O(2)-Ti 107.41(19). Symmetry transformations used to generate equivalent atoms: (a) $-x, -y+1, -z+1$.

gen atoms. This situation is typical, since in the majority of Ti-O-Ti units the individual Ti–μ-O bonds are broadly equivalent. Condensed titanoxanes containing Ti_4O_4 skeleton units are known, for example, [$Ti_4(\mu$-$O)_4Cl_8(MeCN)_8$], and are formed in situ by controlled hydrolysis of titanium species.[13] Continuing these studies we found that reaction of $TiCl_4$ with crude guaiacol in THF gives an air-sensitive reddish-brown crystalline species [$Ti_2(\mu$-$O)Cl_2(\eta^2$-guaiacolato$)_4$] (**7**). The crystal structure of **7** is shown in Figure 6. Each titanium atom is six-coordinated by four oxygen atoms of two guaiacolato ligands, the bridging oxygen atom and terminal chlorine atom. The geometrical parameters are in accordance with those found in **3** and **6**. The coordinative ether oxygen atoms of guaiacolato ligands are located *trans* to the chlorine atoms in **6** and bridging oxygen atoms in **7**.

The Ti-O-Ti bridging oxygen atoms in **6** and **7** result most likely from hydrolysis by adventitious water in the crude guaiacol.[13] It is apparent that solvent and ligand deoxygenation to oxo species is facilitated by impurities such as water Scheme 3.[14, 15]

Controlled hydrolysis of Ti–Cl and Ti–OR bonds is a convenient route to titanoxanes involving either oxo-bridged linkages (Ti-O-Ti) or terminal-bonded titanyl (Ti=O) moieties.[13]

Electrochemical investigations: The electrochemical behaviour of complexes **1, 2** and **4**–**7** (Table 1) was investigated by

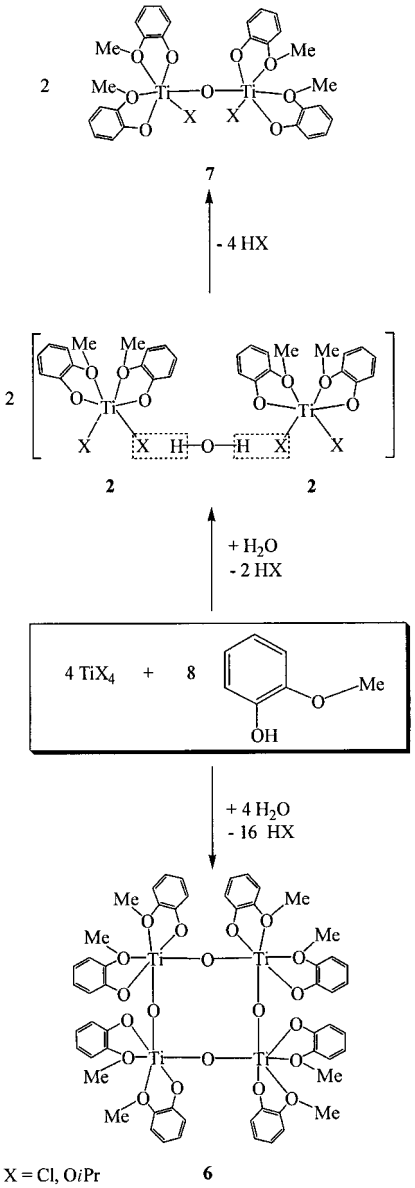

Scheme 3. Controlled hydrolysis reaction of **2** gave the μ-oxo compounds **6** and **7**.

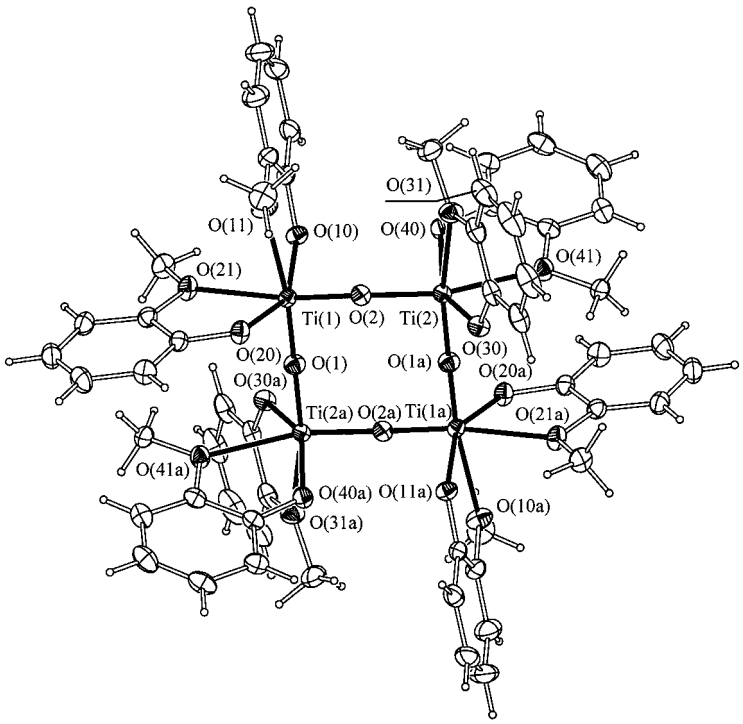

Figure 5. Molecular structure of $[Ti_4(\mu\text{-}O)_4(\eta^2\text{-guaiacolato})_8]\cdot CH_3OH$ (**6**). The displacement ellipsoids are drawn at the 50% probability level. Acetonitrile molecules are omitted for clarity Selected bond lengths [pm] and angles [deg]: Ti(1)–O(1) 180.14(11), Ti(1)–O(2) 181.46(11), Ti(1)–O(10) 190.08(11), Ti(1)–O(20) 190.46(11), Ti(1)–O(21) 227.28(11), Ti(1)–O(11) 228.91(12), Ti(2)–O(1a) 180.49(11), Ti(2)–O(2) 181.19(11), Ti(2)–O(30) 190.11(11), Ti(2)–O(40) 190.26(11), Ti(2)–O(31) 228.63(12), Ti(2)–O(41) 230.94(12), O(1)–Ti(2a) 180.49(11), O(1)-Ti(1)-O(2) 103.47(5), O(1)-Ti(1)-O(10) 98.06(5), O(2)-Ti(1)-O(10) 101.67(5), O(1)-Ti(1)-O(20) 101.26(5), O(2)-Ti(1)-O(20) 97.93(5), O(1)-Ti(1)-O(21) 89.48(5), O(2)-Ti(1)-O(21) 166.19(5), O(1)-Ti(1)-O(11) 168.12(5), O(2)-Ti(1)-O(11) 87.03(5), O(2)-Ti(2)-O(30) 103.38(5), O(2)-Ti(2)-O(40) 97.76(5), O(2)-Ti(2)-O(31) 88.01(5), O(2)-Ti(2)-O(41) 167.96(5), Ti(1)-O(1)-Ti(2a) 177.40(7), Ti(2)-O(2)-Ti(1) 140.09(7). Symmetry transformations used to generate equivalent atoms: (a) $-x+2, -y, -z+1$.

cyclic voltammetry (CV) and controlled potential electrolysis (CPE) in aprotic medium, $[NBu_4][BF_4]$ 0.2 mol dm^{-3}/CH_2Cl_2 (or THF), at a Pt-disc or -gauze electrode, respectively. Although a detailed electrochemical study of those complexes was hampered by their instability in the electrolyte medium, adsorption at the electrode surface and electrode passivation along the CPE experiments, it was possible to observe, in their cyclic voltammograms, both cathodic and anodic waves. The former waves, which are believed (see below) to involve the reduction of Ti^{IV}, are reversible for the mononuclear maltolato complexes **1** and **4**, but irreversible for the dinuclear **5**. They occur at a less cathodic potential ($E_{1/2}^{red}$ about -1.00 V (**1** or **4**) or -1.55 V (**5**) versus SCE) than that for the guaiacolato complexes, whose cathodic waves are observed at $E_p^{red} = -1.94$ (**6**), -2.31 and -2.53 V (**7**) and are irreversible. For the guaiacolato complex **2** no genuine cathodic wave was detected up to the onset of the solvent/electrolyte discharge, whereas its maltolato analogue, **1**, is reduced at $E_{1/2}^{red} = -0.99$ V, that is, at a much less cathodic potential. These observations suggest that the guaiacolato ligand behaves as a considerably stronger electron donor than the ligating maltolato.

In contrast, the chloride and the ethoxide ligands, in the corresponding complexes **1** and **4**, exhibit an identical electron-donor ability as indicated by the identical reduction potentials ($E_{1/2}^{red} = -0.99$ V or -1.00, respectively) or their reversible cathodic waves. For the mononuclear maltolato complexes, the above cathodic waves are replaced gradually by others as a result of the spontaneous conversion of the starting complexes in other species through with ligand liberation; this, therefore, precludes accurate measurements, by CPE, of the numbers of electrons exchanged. Hence, the mononuclear complex **4**, in a mixture with **5** (initial **4**:**5** molar ratio of ca. 3:1), converts into the dinuclear **5** (see Scheme 2), with liberation of maltol, and this conversion, either in solution or in the solid state, was monitored electrochemically as follows. The cyclic voltammogram of a freshly prepared solution of the mixture exhibits a first reversible cathodic wave at $E_{1/2}^{red} = -1.00$ V due to the reduction of **4** and a second

0947-6539/01/0705-0954 $ 17.50+.50/0 *Chem. Eur. J.* **2001**, *7*, No. 5

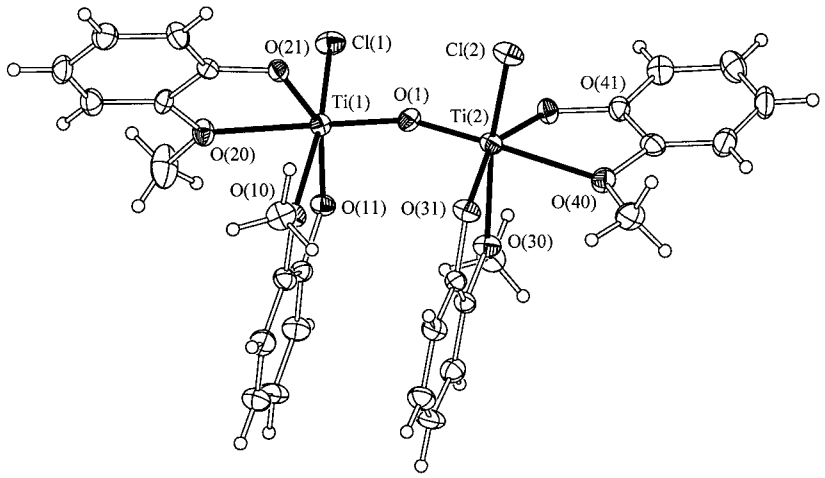

Figure 6. Molecular structure of $[Ti_2(\mu\text{-}O)Cl_2(\eta^2\text{-guaiacolato})_4]$ (**7**). The displacement ellipsoids are drawn at the 50% probability level. Selected bond lengths [pm] and angles [deg]: Ti(1)–Cl(1) 228.40(9), Ti(1)–O(1) 181.79(19), Ti(1)–O(11) 187.88(18), Ti(1)–O(10) 220.40(18), Ti(1)–O(21) 187.49(18), Ti(1)–O(20) 225.78(19), Ti(2)–Cl(2) 226.89(9), Ti(2)–O(1) 177.78(18), Ti(2)–O(31) 188.34(18), Ti(2)–O(30) 220.76(19), Ti(2)–O(41) 188.32(18), Ti(2)–O(40) 227.89(19), O(1)-Ti(1)-O(21) 95.94(8), O(1)-Ti(1)-O(11) 103.73(8), O(1)-Ti(1)-O(10) 91.90(8), O(10)-Ti(1)-O(20) 79.62(7), O(1)-Ti(1)-Cl(1) 99.48(6), O(10)-Ti(1)-Cl(1) 166.82(5), O(1)-Ti(2)-O(31) 103.86(9), O(1)-Ti(2)-O(30) 89.70(8), O(31)-Ti(2)-Cl(2) 94.61(6), O(30)-Ti(2)-Cl(2) 166.33(6), O(1)-Ti(2)-O(40) 167.43(8), Ti(2)-O(1)-Ti(1) 162.11(12).

Table 1. Electrochemical data[a] for the titanium complexes **1, 2** and **4**–**6**.

	E_p^{red} ($E_{1/2}^{red}$)	n	E_p^{ox}
1	−0.76 (*−0.99*)[b]	1.0[c]	1.50
2	[d]		1.55[e]
4[f]	(−1.00)[g]	[h]	1.47[i]
5[f]	−1.55		
6	−1.94[j]	3.5	1.54[k]
7	*−2.31*[l]	1.8[n]	1.53[e]
	−2.53[m]		
maltol[o]	−2.06[p]		1.73[q]
guaiacol[o]			1.55[r]

[a] In$[NBu_4][BF_4]$ 0.2 mol dm^{-3}/CH_2Cl_2, unless stated otherwise; values of peak potentials (E_p) for irreversible waves or of half-wave potential ($E_{1/2}$ in brackets) for reversible ones are given in volt ±0.02 vs. SCE, measured at a scan rate of 0.20 V s^{-1}; when one wave predominates over the others, its redox potential is given in italics; n = number of electrons (as measured by CPE) per molecule of complex (the values in the column correspond to the cathodic waves). [b] This wave decreases in intensity with time, being replaced by that at $E_p^{red} = -0.76$ V (which becomes the predominant one) and by another one, of lower current intensity, at −0.52 V. [c] Overall number of electrons, for all the cathodic waves. [d] A cathodic wave, initially not observed, develops at $E_p^{red} = -1.8$ V after a few CV scans. [e] Current function is approximately four times that of the free guaiacol. [f] In a mixture of **4** and **5**, with predominance (ca. 3:1) of the former. [g] This wave is replaced by others at $E_p^{red} = -1.55$ and −2.06 V, the former being assigned to complex **5** and the latter to free maltol. [h] Not possible to measure due to decomposition. [i] This wave is replaced by another one at $E_p^{ox} = 1.73$ V assigned to free maltol; the overall current function for these two anodic waves is about twice that of free maltol, and they involve an overall number of two electrons (measured by anodic CPE in NCMe); after CPE at any of these anodic waves ($n = 0.3$ electrons for the first one), a new cathodic wave is observed at −1.0 V. [j] In THF; a new anodic wave is detected at $E_p^{ox} = 0.02$ V upon scan reversal following the CV cathodic sweep or upon the cathodic CPE. [k] Current-function about eight times that of free guaiacol. [l,m] In THF; an anodic wave is detected at $E_p^{ox} = -1.96$ or −1.22 V, respectively, upon scan reversal. [n] A new anodic wave is observed at $E_p^{ox} = -0.09$ V after the cathodic CPE. [o] Included for comparative purposes. [p] In DMSO. [q] A new cathodic wave is observed at $E_p^{red} = -1.45$ V after the anodic CPE ($n = 1$ electron). [r] $n = 1.2$ electrons, as measured by anodic CPE.

irreversible one at $E_p^{red} = -1.55$ V (with the expected peak current ratio relative to the former wave) assigned to the reduction of the dinuclear species **5**. The former wave is progressively replaced by the latter one and as well by another one at $E_p^{red} = -2.06$ V, due to the reduction of liberated maltol. The anodic behaviour of the solution (see below) is also consistent with the conversion of **4** to **5** in the electrolyte solution. Moreover, the occurrence of this partial dimerisation, although slower, in the solid state, was also indicated by the corresponding changes in the cyclic voltammogram of the above sample of **4** + **5** after being kept in the solid state under dinitrogen for about two months.

The reversible cathodic wave of the chloromaltolato complex **1**, in the electrolyte solution at $E_{1/2}^{red} = -0.99$ V is also replaced by other cathodic waves at $E_p^{red} = -0.76$ V (which becomes the dominant one) and −0.52 V. These values are within the range observed for the $Ti^{IV} \rightarrow Ti^{III}$ reduction potential of other polychloro–Ti^{IV} complexes[17] such as $[TiCl_6]^{2-}$ (−0.95 V), $[TiCl_5(THF)]^-$ (−0.75 V) or $[TiCl_4(\mu\text{-}Cl)_2Mg(THF)_4]$ (−0.56 V). As measured by CPE, the overall number of electrons for all the above cathodic waves exhibited by the electrolyte solution of **1** is one per titanium atom; this also suggests the involvement of $Ti^{IV} \rightarrow Ti^{III}$ processes. CPE at the first cathodic wave of the dinuclear complex **7**, as well as at the cathodic wave of the tetranuclear complex **6**, also indicated the exchange of one electron per Ti^{IV}.

The cathodic processes of our complexes are not expected to occur at the ligands, since free maltol is reduced only at a much more cathodic potential value ($E_p^{red} = -2.1$ V) than those of the maltolato complexes **1**, **4** and **5** and, moreover, no cathodic wave was found for guaiacol down to the solvent–electrolyte discharge potential. This and the above observations can be accounted for by considering that the cathodic processes are centred at the metal sites, involving the reduction of Ti^{IV} to Ti^{III} ions.

In contrast, the irreversible anodic waves observed by CV for our Ti^{IV} complexes should be centred at the maltolato or guaiacolato ligands. In fact, they occur at oxidation potentials (E_p^{ox} about 1.5 V) that are comparable with those observed for the free ligands ($E_p^{ox} = 1.73$ or 1.55 V for maltol or guaiacol respectively, the latter value being similar to that reported,[18] 1.49 V, for the oxidation of 4-methoxyphenol). Moreover, in agreement with the presence of various redox-active maltolato or guaiacolato ligands in each molecule of the complexes, the anodic current functions for the latter ($i_p/(v^{1/2}c)$, in which i_p = peak current, v = scan rate, c = concentration of complex)

are much higher then those of the corresponding free maltol or guaiacol. Hence, for example the current functions of the anodic waves exhibited by solutions of complexes **7** and **6**, with four or eight guaiacolato ligands, respectively, are roughly four or eight times the current function of guaiacol.

The dimerisation of complex **4** with liberation of maltol (see below) was also supported by the observed anodic behaviour, in particular the appearance of an irreversible oxidation wave at the same potential ($E_p^{ox} = 1.73$ V) as that measured for free maltol, with a concomitant decrease of the peak current of the genuine anodic wave (at $E_p^{ox} = 1.47$ V) of the complex. The sum of the current functions of those two anodic waves is roughly twice the current-function of free maltol, in accord with the above observations for the guaiacolato complexes. Moreover, the overall number of electrons exchanged per Ti atom in those two anodic processes, as measured by CPE at the peak potential of the second anodic wave, is two, that is, the expected value for the involvement of the oxidation of two maltolato and/or maltol species (a single electron is exchanged in the anodic CPE of free maltol at its anodic wave). However, the number of electrons exchanged at the genuine anodic wave ($E_p^{ox} = 1.47$ V) of complex **4** (as measured by CPE at this wave) is only 0.3 electrons per complex molecule; this indicates that during the time of the electrolysis most of the complex converted into other species with liberation of maltol. Such an instability also precluded the measurement of the number of electrons exchanged in the cathodic process.

Polymerisation studies: The results of an ethylene polymerisation test on the six related titanium maltolato and guaiacolato complexes **1, 2** and **4**–**7** are shown in Table 2.

Table 2. Polymerisation[a] of ethylene with a Ti-$MgCl_2$-$AlEt_3$/$AlEt_2Cl$ catalyst.

	Productivity[b]
1	345
2	22
4	210
5	177
6	78
7	580

[a] Polymerisation conditions: $[Ti]_0 = 0.01$ mmol dm^{-3}, Al:Ti = 500:1, Mg:Ti = 10:1, $P_{ethylene} = 0.5$ Mpa, in hexane. [b] Mass in kilograms of polymer formed per gram of titanium atom in 1 h.

The catalyst was prepared by milling a hexane slurry of $MgCl_2$ and one of these compounds. Triethylaluminium and $AlEt_2Cl$ were used as cocatalysts. The highest activities were obtained with [$Ti_2(\mu$-O)Cl_2(guaiacolato)$_4$] (**7**) and *cis*-[$TiCl_2$(maltolato)$_2$] (**1**), corresponding to 580 and 345 kg polyethylene per gram of Ti per hour ($[Ti]_0 = 0.01$ mmol dm^{-3} and [Al] = 5 mmol dm^{-3}), respectively. In contrast, 22 and 131 kg polyethylene per gramme of Ti per hour were obtained under the same conditions when monomeric [$TiCl_3(THF)_3$] and dimeric [$Ti_2(\mu$-Cl)$_2Cl_4(THF)_4$] were used as procatalysts, respectively.[19]

Conclusion

A new class of titanium compounds **1**–**7** has been developed which, with $AlEt_3$ and $AlEt_2Cl$, are active for the polymerisation of ethylene. The class of [L_2TiCl_2] (L = η^2-maltolato or η^2-guaiacolato) systems can be used as a valuable alternative for the well-documented range of Group 4 metallocenes.[1] The electrochemical studies (Table 1) indicate that the maltolato ligand behaves as a weaker electron donor than guaiacolato (less cathodic reduction potentials for the maltolato complexes), forms less stable mononuclear Ti^{IV} complexes in the electrolyte solution (e.g., dimerisation occurs with liberation of maltol), but stabilises the Ti^{III} complexes derived on reduction better (reversible cathodic waves for the maltolato complexes, but irreversible for the guaiacolato ones). However, the ethoxide and the chloride ligands exhibit identical electron-donor characters in the mononuclear complexes. These results also allow us to get an insight towards the clarification of some aspects of the titanium-catalysed ethylene polymerisation. The compounds [$Ti_2(\mu$-O)$Cl_2(\eta^2$-guaiacolato)$_4$] (**7**) and *cis*-[$TiCl_2(\eta^2$-maltolato)$_2$] (**1**) show a much higher catalytic activity in ethylene polymerisation with respect to the other complexes (Table 2), and the different nature of the maltolato and guaiacolato ligands surprisingly only results, for these systems, in a weak effect on the catalyst activity; however, the replacement of maltolato by guaiacolato in the mononuclear complexes leads to quite a significant reduction in the activity (compare complexes **2** and **1**). A decrease of the catalytic activity also results from replacement of chloride by ethoxide ligands (compare **1** with **4**), in spite of their identical electron-donor abilities. The lability of the maltolato and guaiacolato ligands towards liberation from the titanium centres (as observed in the electrochemical studies) accounts for their replacement during the catalyst preparation, and the aluminium cocatalyst conceivably behaves as the ligand abstracting agent[19] and chloride donor to the active metal site. How all the compounds are incorporated in the catalyst can only be answered by further studies.

Experimental Section

Materials and methods: All the syntheses were performed under a dry dinitrogen atmosphere by using standard Schlenk techniques. Solvents were dried and then distilled under N_2 by following conventional methods. Maltol, guaiacol, $TiCl_4$, $AlMe_3$, $AlEt_2Cl$ were purchased from Aldrich. IR spectra were measured on a Perkin-Elmer 180 instrument in Nujol mulls. NMR spectra were performed on a Bruker ESP 300E spectrometer. The electrochemical experiments were performed on an EG & G PAR 273 potentiostat/galvanostat connected to a PC through a GPIB interface. Cyclic voltammetry (CV) was undertaken in a two-compartment three-electrode cell, with a platinum-disc ($d = 0.5$ mm) working electrode, probed by a Luggin capillary connected to silver-wire pseudo-reference electrode; a platinum auxiliary electrode was employed. Controlled potential electrolysis (CPE) was carried out in a two-compartment three-electrode H-type cell with platinum-gauze working and counter electrodes in compartments separated by a glass frit; a Luggin capillary, probing the working electrode, was connected to a silver-wire pseudo-reference electrode. Frequent interruption of the electrolyses was commonly required for cleaning the working electrode surface, due to its passivation. The experiments were performed under dinitrogen at room temperature, the potentials were measured in 0.2 mol dm^{-3} [NBu_4][BF_4]/CH_2Cl_2 (THF or

0947-6539/01/0705-0956 $ 17.50+.50/0 *Chem. Eur. J.* **2001**, *7*, No. 5

DMSO for maltol) and are quoted relative to the saturated calomel electrode (SCE) by using as internal reference the $[Fe(\eta^5\text{-}C_5H_5)_2]^{0/+}$ couple ($E^{ox}_{1/2} = 0.525$, 0.545 or 0.440 V *vs.* SCE, respectively). The CPE experiments were monitored regularly by CV, thus assuring that no significant potential drift occurred during the electrolyses.

Compound 1: Maltol (2.29 g, 18.22 mmol) was added to a stirred solution of $TiCl_4$ (1.73 g, 9.11 mmol) in toluene (60 mL) at room temperature. The reaction mixture turned orange-red. After 24 h, the volume was reduced to 20 mL under vacuum, and hexane (50 mL) was added to give an orange precipitate, which was filtered off, washed with hexane (3 × 5 mL) and dried under vacuum. The solid was recrystallised from CH_2Cl_2/THF (3:1) to yield orange-red crystals. Yield 3.0 g (89 %); ^{1}HNMR (300 MHz, $CDCl_3$): $\delta = 8.09$ (d, 1H; 6-*H*C_5H_2O), 6.64 (d, 1H; 5-*H*C_5H_2O), 2.50 (s, 3H; C*H*$_3$); IR (CsI, Nujol): $\tilde{\nu} = 280$ (m), 382 (vs), 524 (m), 564 (m), 640 (m), 740 (vs), 834 (s), 934 (s), 1036 (s), 1094 (s), 1094 (s), 1198 (s), 1266 (s), 1540 (vs), 1610 cm^{-1} (s); elemental analysis calcd (%) for $C_{12}H_{10}O_6Cl_2Ti$ (367.93): C 39.02, H 2.71, Cl 19.24, Ti 13.02; found C 39.84, H 2.24, Cl 18.85, Ti 12.75.

Compound 2: Freshly distilled guaiacol (2.27g, 18.22 mmol) was added to a solution of $TiCl_4$ (1.73g, 9.11 mmol) in toluene (60 mL). The brown-orange mixture was stirred at room temperature. After 24 h, the volume was reduced to 40 mL, and the redish-brown precipitate was filtered off, washed with toluene (3 × 5 mL) and dried under vacuum. Crystals suitable for the structure determination were obtained from post-reaction mixture after one week. Yield 2.62 g (80 %); ^{1}HNMR (300 MHz, $CDCl_3$): $\delta = 7.02$ (m, 1H; 4-*H*Ar), 6.89 (m, 2H; 3,6-HAr), 6.71 (m, 1H; 5-*H*Ar), 4.02 (s, 3H; OC*H*$_3$); IR (CsI, Nujol): $\tilde{\nu} = 406$ (s), 440 (w), 472 (m), 570 (vw), 640 (w), 664 (s), 750 (s), 756 (s), 860 (m), 930 (w), 996 (s), 1018 (m), 112 (m), 1156 (w), 1160 (m), 1208 (m), 1248 (vs), 1252 (s), 1270 (m), 1324 (m), 1584 cm^{-1} (w); elemental analysis calcd (%) for $C_{14}H_{14}O_4Cl_2Ti$ (363.97): C 46.03, H 3.83, Cl 19.45, Ti 13.15; found C 45.48, H 4.02, Cl 18.93, Ti 12.87.

Compound 3: Maltol (0.4 6 g, 3.36 mmol) was added to a solution of $[Ti(O\textit{i}Pr)_4]$ (1.00 g, 3.36 mmol) in THF (45 mL). The light yellow mixture was stirred at room temperature for 12 h, then the volatiles were removed in vacuum. The light yellow solid was washed with hexane (40 mL), and then the white precipitate was filtered off, washed with hexane (3 × 5 mL) and dried under vacuum. Yield 1.15 g (82 %); IR (CsI, Nujol): $\tilde{\nu} = 326$ (w), 352 (s), 368 (s), 384 (s), 474 (vs), 544 (m), 620 (s), 726 (m), 786 (w), 842 (s), 928 (w), 980 (s), 1124 (s), 1198 (s), 1240 (s), 1282 (vs), 1326 (m), 1580 (s), 1594 cm^{-1} (vs); elemental analysis calcd (%) for $C_{18}H_{24}O_8Ti$ (416.09): C 51.89, H 5.76, Ti 11.53; found C 50.72, H 5.53, Ti 12.08.

Compound 4: Maltol (0.85 g, 6.72 mmol) was added to a solution of $[Ti(O\textit{i}Pr)_4]$ (1.00 g, 3.36 mmol) in THF (45 mL). The light yellow mixture was stirred at room temperature for 12 h, then the volatiles were removed in vacuum. The resulting light yellow solid was recrystallised from ethyl acetate to yield yellow crystals. Yield 0.83 g (74 %); ^{1}HNMR (300 MHz, $CDCl_3$): $\delta = 7.74$ (d, 1H; 6-*H*C_5H_2O), 6.40 (d, 1H; 5-*H*C_5H_2O), 4.45 (q, 2H; OC*H*$_2$CH$_3$), 2.19 (s, 3H; C*H*$_3$), 1.17 (t, 3H; OCH$_2$C*H*$_3$); IR (CsI, Nujol): $\tilde{\nu} = 304$ (w), 388 (s), 478 (s), 548 (s), 620 (s), 726 (s), 766 (m), 832 (s), 916 (s), 1062 (m), 1104 (s), 1196 (m), 1244 (m), 1278 (vs), 1508 (s), 1576 cm^{-1} (vs); elemental analysis calcd (%) for $C_{16}H_{20}O_8Ti$ (388.06): C 49.25, H 5.23, Ti 12.14; found C 48.93, H 5.98, Ti 12.98.

Compound 5: Crystalline compound **4** (0.5 g, 1.29 mmol) was dissolved in a mixture of THF (30 mL) and ethyl acetate (10 mL) and left to crystallise at room temperature. After 3 days the plate-shaped yellow crystals were filtered off and washed with hexane (3 × 5 mL). Yield 0.18 g (45 %); ^{1}HNMR (300 MHz, $CDCl_3$): $\delta = 7.77$ (d, 1H; 6-*H*C_5H_2O), 6.47 (d, 1H; 5-*H*C_5H_2O), 4.52 (q, 2H; μ-OC*H*$_2$CH$_3$), 3.70 (q, 4H; OC*H*$_2$CH$_3$), 2.42 (s, 3H; C*H*$_3$), 1.25 (m, 9H; OCH$_2$C*H*$_3$, μ-OCH$_2$C*H*$_3$); IR (CsI, Nujol): $\tilde{\nu} = 284$ (w), 356 (w), 410 (m), 466 (s), 544 (s), 628 (m), 726 (s), 802 (s), 854 (s), 926 (m), 1040 (w), 1090 (w), 1128 (w), 1204 (s), 1276 (vs), 1516 (s), 1584 cm^{-1} (vs); elemental analysis calcd (%) for $C_{24}H_{40}O_{12}Ti_2$ (616.15): C 46.75, H 6.49, Ti 15.58; found C 47.23, H 5.98, Ti 15.32.

Compound 6: Guaiacol (0.9 g, 7.28 mmol) was added to a solution of $[Ti(O\textit{i}Pr)_4]$ (1.00 g, 3.36 mmol) in THF (40 mL). The reaction mixture turned yellow and was stirred at room temperature. After 12 h, volatiles were removed in vacuum, and the resulting yellow solid was recrystallised from acetonitrile to yield yellow crystals. Yield 0.62 g (55 %); ^{1}HNMR (300 MHz, CD_3CN): $\delta = 6.93$ (m, 1H; 4-*H*Ar), 6.81 (m, 2H; 3,6-*H*Ar), 6.46 (m, 1H; 5-*H*Ar), 3.83 (s, 3H; OC*H*$_3$); IR (CsI, Nujol): $\tilde{\nu} = 378$ (w), 464 (m), 644 (s), 738 (vs), 856 (s), 1010 (s), 1108 (vs), 1260 (vs), 1280 (vs), 1596 (m), 1752 (vw), 1868 (vw), 1912 cm^{-1} (vw); elemental analysis calcd (%) for $C_{56}H_{56}O_{20}Ti_4$ (1240.13) (the yellow product before recrystallization from acetonitrile): C 54.24, H 4.52, Ti 15.43; found C 55.13, H 4.76, Ti 16.01.

Compound 7: Crude guaiacol (2.27 g, 18.22 mmol) was added to a solution of $TiCl_4$ (1.73 g, 9.11 mmol) in THF (60 mL). The brown-orange mixture was stirred at room temperature. After 24 h, the volume was reduced to 40 mL, and the reddish-brown precipitate was filtered off, washed with toluene (3 × 5 mL) and dried under vacuum. Crystals suitable for the structure determination were obtained from post-reaction mixture after one week. Yield 2.54 g (82 %); ^{1}HNMR (300 MHz, C_6D_6): $\delta = 6.84$ (m, 1H; 4-*H*Ar), 6.62 (m, 2H; 3,6-*H*Ar), 6.15 (m, 1H; 5-*H*Ar), 3.42 (s, 3H; OC*H*$_3$); IR (CsI, Nujol): $\tilde{\nu} = 334$ (vw), 364 (w), 406 (vs), 442 (s), 472 (vs), 544 (w), 562 (w), 584 (w), 626 (m), 640 (s), 664 (vs), 750 (vs), 760 (vs), 774 (vs), 832 (m), 858 (vs), 920 (w), 996 (vs), 1028 (vs), 1110 (vs), 1154 (m), 1172 (s), 1208 (s), 1248 (vs), 1276 (s), 1324 (s), 1582 (m), 1600 cm^{-1} (w); elemental analysis calcd (%) for $C_{28}H_{28}O_9Cl_2Ti_2$ (674.01): C 49.80, H 4.15, Cl 10.5, Ti 14.19; found C 49.53, H 4.28, Cl 11.2, Ti 13.94.

Polymerisation test: A slurry of $MgCl_2$ (30 mmol) in hexane was milled under argon in a glass mill (capacity 250 mL, with 20 balls of diameter 5–15 mm) at room temperature for 6 h. Then titanium compound (3 mmol) and hexane (50 mL) were added, and the mixture was milled for 24 h. The sample of procatalyst suspension (containing 0.01 % titanium) was activated with $AlEt_3$/$AlEt_2Cl$ (1:1 molar ratio; 20 mmol) for 15 min at 323 K under argon to form a highly active catalyst. The polymerisation of ethylene was carried out at 323 K in a stainless steel reactor (1 dm^3), equipped with a stirrer, in hexane at 0.6 MPa ethylene pressure. The polymerisation was quenched with a 5 % solution of HCl in methanol (150 mL), and the polymer was filtered off, washed with methanol and dried under vacuum.

Crystallography: Preliminary examination and intensities data collections were carried out on a KUMA KM4 four-circle diffractometer[21] for **5** (radiation $Mo_{K\alpha}$, $\lambda = 0.71073$), and KUMA KM4 CCD four-circle diffractometer[22] with an Oxford Cryosystem-Cryostream cooler for compounds **2**, **4**, **6** and **7** (radiation $Mo_{K\alpha}$, $\lambda = 0.71073$). Details of the data collection, refinement and crystal data are summarised in Table 3. All data were corrected for Lorentz and polarisation effects. After refinement with isotropic displacement parameters for all atoms, an absorption correction based on least-squares fitted against $|F_c| - |F_o|$ differences was also applied[23] to the data of **2**, **5** and **7**. The structures were solved by direct methods (SHELXS 97)[24] and refined by full-matrix least-squares on F^2 using SHELXL 97[25]. Non-hydrogen atoms were refined with anisotropic thermal parameters. The carbon-bonded hydrogen atoms were included in the calculated positions and refined by using a riding model with isotropic displacement parameters equal to 1.2 U_{eq} of the attached atom. In the structure of **5**, one methyl C atom of ethoxide group (O(1)) was disordered and was modelled using two sets of sites with 0.58 occupancy. Scattering factors were taken from the literature.[26] Crystallographic data (excluding structure factors) for the structures reported in this paper have been deposited with the Cambridge Crystallographic Data Centre as supplementary publication no. CCDC-154577 to CCDC-154581. Copies of the data can be obtained free of charge on application to CCDC, 12 Union Road, Cambridge CB2 1EZ, UK (fax: (+44) 1223-336-033; e-mail: deposit@ccdc.cam.ac.uk).

Acknowledgements

The authors thank the State Committee for Scientific Research (Poland) (grant No 3 T09A03517), as well as the Fundação para a Ciência e a Tecnologia (FCT) and the PRAXIS XXI Programme (Portugal).

[1] R. F. Jordan, *Adv. Organomet. Chem.* **1991**, *32*, 325; T. J. Marks, *Acc. Chem. Res.* **1992**, *25*, 57; J. A. Ewen, *J. Am. Chem. Soc.* **1984**, *106*, 6355; W. Kaminsky, K. Külper, H. H. Brintzinger, F. R. W. P. Wild, *Angew. Chem.* **1985**, *97*, 507; *Angew. Chem. Int. Ed. Engl.* **1985**, *24*, 507; H. H. Brintzinger, D. Fischer, R. Mülhaupt, B. Rieger, R. Waymouth, *Angew. Chem.* **1995**, *107*, 1255 (1652); *Angew. Chem. Int. Ed. Engl.* **1995**, *34*, 1143 (1368).

Table 3. Crystal data and structure refinement for **2**, and **4**–**7**.

	2	**4**	**5**	**6**	**7**
formula	$2(C_{14}H_{14}Cl_2O_4Ti)$	$C_{16}H_{20}O_8Ti$	$(C_{12}H_{20}O_6Ti)_2$	$C_{56}H_{66}O_{29}Ti_4$, $4(CH_3CN)$	$C_{28}H_{28}Cl_2O_9Ti_2$
M_r	730.10	388.22	616.24	1404.82	675.20
crystal system	triclinic	triclinic	monoclinic	triclinic	monoclinic
space group	$P\bar{1}$	$P\bar{1}$	$P2_1/n$	$P\bar{1}$	$P2_1/c$
a [Å]	9.446(1)	8.186(1)	9.418(2)	11.0335(8)	13.803(1)
b [Å]	12.490(1)	8.347(1)	11.609(2)	12.3068(8)	21.287(2)
c [Å]	14.198(1)	12.757(1)	14.544(3)	12.7609(9)	9.970(1)
α [°]	90.31(1)	89.87(3)		72.287(6)	
β [°]	102.08(1)	84.86(3)	94.51(3)	88.254(6)	92.06
γ [°]	107.46(1)	87.48(3)		81.453(6)	
V [Å^3]	1558.3(2)	867.32(16)	1585.2(5)	1632.1(2)	2927.5(5)
Z	2	2	2	1	4
crystal size [mm]	$0.5 \times 0.4 \times 0.2$	$0.4 \times 0.2 \times 0.2$	$0.6 \times 0.4 \times 0.3$	$0.6 \times 0.5 \times 0.4$	$0.6 \times 0.4 \times 0.4$
ρ_{calcd} [g cm^{-3}]	1.556	1.487	1.291	1.429	1.532
μ [mm^{-1}]	0.902	0.534	0.557	0.548	0.780
$F(000)$	744	404	648	728	1384
scan mode	ω	ω	ω-2θ	ω	ω
T [K]	100.0(5)	100.0(5) K	299(2)	100.0(5)	100.0(5)
max 2θ [°]	57.0	57.6	50	57.6	57.4
reflections	10513	6208	2524	11623	18345
unique reflections	6758	3908	2409	7371	6706
observed reflections [$I > 2\sigma(I)$]	5395	2783	1657	6291	3873
parameters	383	230	184	421	374
$R(F)$ for $I > 2\sigma(I)$]	0.0440	0.0319	0.0503	0.0344	0.0421
$wR2(F^2)$ for all data	0.1314	0.0800	0.1619	0.0930	0.0898
goodness of fit on F^2	1.116	1.0	1.078	1.037	0.891
largest diff. peak/ hole [e Å^3]	0.802/ − 0.428	0.587/ − 0.374	0.548/ − 0.309	0.348/ − 0.423	0.437/ − 0.348

[2] M. Kakugo, T. Miyatake, K. Mizunuma, *Chem. Express* **1987**, *2*, 445; T. Miyatake, K. Mizunuma, Y. Seki, M. Kakugo, *Makromol. Chem. Rapid Commun.* **1989**, *10*, 349; T. Miyatake, K. Mizunuma, and M. Kakugo, *Makromol. Chem. Macromol. Symp.* **1993**, *66*, 203; W. Kaminsky, *Catal. Today* **1994**, *20*, 257; M. Shmulinson, M. Galan-Fereres, A. Lisovskii, E. Nelkenbaum, R. Semiat, M. S. Eisen, *Organometallics* **2000**, *19*, 1208.

[3] J. Schaverien, A. J. Van der Linden, A. G. Orpen, *Polym. Prepr.* **1994**, *35*, 672; C. J. Flores, C. J. W. Chen, M. D. Rausch, *Organometallics* **1995**, *14*, 1827; C. J. Flores, C. J. W. Chen, M. D. Rausch, *Organometallics* **1995**, *14*, 2106; H. Furann, S. Brenner, P. Arndt, R. Kempe, *Inorg. Chem.* **1996**, *35*, 6742; T. H. Warren, R. R. Schrock, W. M. Davis, *Organometallics* **1996**, *15*, 562; R. Baumann, W. M. Davis, R. R. Schrock, *J. Am. Chem. Soc.* **1997**, *119*, 3830;

[4] A. J. Van der Linden, C. J. Schaverien, M. Meijboom, C. Ganter, A. G. Orpen, *J. Am. Chem. Soc.* **1995**, *117*, 3008.

[5] J. A. Heppert, S. D. Dietz, T. J. Boyle, F. Takusagawa, *J. Am. Chem. Soc.* **1989**, *111*, 1503; T. J. Boyle, D. L. Barnes, J. A. Heppert L. Morales, F. Takusagawa, J. W. Connolly, *Organometallics* **1992**, *11*, 1112; C. Krüger, R. Mynott, C. Siedenbiedel, L. Stehling, G. Wilke, *Angew. Chem.* **1991**, *103*, 1714; *Angew. Chem. Int. Ed. Engl.* **1991**, *30*, 1668.

[6] P. Sobota, S. Szafert, *Inorg. Chem.* **1996**, *35*, 1778.

[7] M. G. Stanton, C. B. Allen, R. M. Kissling, A. L. Lincoln, M. R. Gagne, *J. Am. Chem. Soc.* **1998**, *120*, 5981.

[8] J. Otera, *J. Chem. Rev.* **1993**, *93*, 1449; J. Chin, *J. Acc. Chem. Res.* **1991**, *24*, 145; G. W. Parshall and S. D. Ittel, *Homogeneous Catalysis,* 2nd ed., Wiley, New York, **1992**, pp. 269–280.

[9] P. Sobota, J. Utko, S. Szafert, K. Szczegot, *J. Chem. Soc. Dalton Trans.* **1997**, 679.

[10] P. Sobota, S. Szafert, J. Utko, T.Lis, *J. Organomet. Chem.* **1992**, *423*, 195.

[11] P. Sobota, M. Wróblewska, S. Szafert, T. Głowiak, *J. Organomet. Chem.* **1994**, *481*, 57.

[12] J. Okuda, E. Herdtweck, *Inorg. Chem.* **1991**, 30, 1516.

[13] G. R. Willey, J. Palin, M. G. B. Drew, *J. Chem. Soc. Dalton Trans.* **1994**, 1799 and references therein.

[14] R. C. Mehrotra, A. Singh, *Chem. Soc. Rev.* **1996**, *25*, 1.

[15] W. A. Herrman, N. W. Huber, O. Runte, *Angew. Chem.* **1995**, *107*, 2371; *Angew. Chem. Int. Ed. Engl.* **1995**, *34*, 2187; K. G. Caulton, L. G. Hubert-Pfalzgraf, *Chem. Rev.* **1990**, *90*, 969; D. J. Teff, J. C. Huffman, K. G. Caulton, *J. Am. Chem. Soc.* **1996**, *118*, 4030.

[16] Y. Le Page, J. D. McCowan, B. K. Hunter, R. D. Heyding, *J. Organomet. Chem.* **1980**, *193*, 201; S. Circelos, T. Cuenca, J. C. Flores, R. Gomez, P. Gomez-Sal, P. Royo, *Organometallics* **1993**, *12*, 994; P. Klein, U. Thewalt, K. Doppert, R. Sanchez-Delgado, *J. Organomet. Chem.* **1982**, *236*, 189; T. Klapötke, J. Pickardt, *J. Organomet. Chem.* **1990**, *393*, 343; A. Feltz, *Z. Anorg. Allg. Chem.* **1963**, *323*, 35.

[17] L. M. D. Ribeiro, M. A. N. D. A. Lemos, A. J. L. Pombeiro, P. Sobota, *Russ. J. Electrochem.* **1995**, *31*, 1009.

[18] O. Hammerich, V. D. Parker, A. Ronlán, *Acta Chem. Scand. Ser. B* **1976**, *30*, 89.

[19] P. Sobota, J. Ejfler, S. Szafert, K. Szczegot, W. Sawka-Dobrowolska, *J. Chem. Soc. Dalton Trans.* **1993**, 2353.

[20] Y. Ma, D. Reardon, S. Gambarotta, G. Yap, *Organometallics* **1999**, *18*, 2773.

[21] *Kuma Diffraction. Kuma KM4 System Software. User's Guide, Version 6.1*, Kuma Diffraction, Wrocław, Poland, **1996**.

[22] *Kuma Diffraction. KM4CCD SYSTEM SOFTWARE. User's Guide, Version 1.161*, Kuma Diffraction, Wrocław (Poland) **1995**–**1999**.

[23] P. Starynowicz, *COSABS99: Program for Absorption Correction*, University of Wrocław, Poland, **1999**.

[24] G. M. Sheldrick, *Acta Crystallogr. Sect. A* **1990**, *46*, 467.

[25] G. M. Sheldrick, *SHELXL 97, Program for the Refinement of Crystal Structures*, University of Göttingen (Germany) **1997**.

[26] D. T. Cromer, J. T. Waber in *International Tables for X-ray Crystallography, Vol. IV* (Eds.: J. A. Ibers, W. C. Hamilton), Kynoch, Birmingham (UK) **1974**.

Received: June 23, 2000 [F2562]

0947-6539/01/0705-0958 $ 17.50+.50/0